Applied Biological Research 25(4): 437-446; (2023)
DOI: 10.5958/0974-4517.2023.00049.6

STARCH-BASED ELECTROSPUN NANOFIBROUS SCAFFOLD INCORPORATED WITH BIOACTIVE COMPOUND FROM *Cayratia trifolia* PROMOTES WOUND HEALING BY ACTIVATING VEGF AND PDGF SIGNALING PATHWAYS

Bhuvaneswari Meganathan and Mani Panagal*

Department of Biotechnology, Annai College of Arts and Science (Affiliated by Bharathidasan University), Kovilacheri - 612 503, Tamil Nadu (India)
*****e-mail: *master.maniji@gmail.com*

(Received 26 August, 2023; accepted 27 September, 2023)

ABSTRACT

This study focused on the development of starch-based nanofibrous scaffolds incorporated with linolenyl alcohol derived from ethanolic extracts of *Cayratia trifolia* to enhance wound healing. Electrospun nanofibers were fabricated by blending different concentrations of linolenyl alcohol (10, 20, and 40% v/v) with starch solutions. The resulting nanofibers were characterized for their morphology, size distribution, thermal stability, FT-IR spectra, and wound healing properties. The nanofibers loaded with linolenyl alcohol exhibited diameters ranging from 73 to 95 nm. Further, these nanofibers displayed improved thermal stability compared to free linolenyl alcohol. FT-IR analysis confirmed the interaction between starch and linolenyl alcohol. When 40% linolenyl alcohol-loaded nanofibers were applied, HaCat cells exhibited increased viability. Western blot analysis revealed elevated levels of vascular endothelial growth factor (VEGF) and platelet-derived growth factor (PDGF) expression, suggesting that the developed nanofibers have the potential to promote angiogenesis and cell proliferation, thus facilitating wound healing. In conclusion, our study demonstrated that electrospun starch-based nanofibrous scaffolds incorporating linolenyl alcohol can effectively accelerate wound healing by activating VEGF and PDGF signaling pathways.

Keywords: Electrospinning, linolenyl alcohol, PDGF, starch, VEGF. wound healing

INTRODUCTION

Wound are classified either as acute or chronic depending on how long it takes to them to heal. Hemostasis, inflammation, proliferation, and remodelling are the four stages of normal wound healing (Palanisamy *et al*., 2023). This process must be followed in correct order and duration for a wound to heal completely. The wound normally forms clots immediately after an injury is detected. This not only prevents excessive blood loss but also prevent microbes from entering into the body through laceration (Pei *et al.,* 2023). During the 2nd phase of healing, inflammatory cells are sent to the wound site by the body in response to sudden injury. The injured area may become swollen, red, hot, and painful. In the proliferative phase, new blood vessels and tissues are formed through angiogenesis, which overlaps the inflammatory stage. In addition, extracellular matrix is constructed to fill in the wound. In contrast, the remodelling phase involves the maturation of extracellular matrices into scars and an increase in their tensile strength at the end of wound healing. Additionally, their aggregation into larger blood vessels reduces the number of capillaries (Xu *et al.*, 2020).

It is common for chronic wounds or those wounds that refuse quick healing to follow a prolonged and generally incomplete recovery process. There are several pathological conditions that can result in non-healing wounds, including diabetes, obesity, and even stressful environmental conditions. During persistent inflammatory phases, granular tissue formation can be obstructed in diabetic patients (Pei *et al.,* 2022). Many diabetic patients suffer from peripheral neuropathy, which is a loss of sensation in the peripheral nervous system. Since affected individuals are unable to feel pain or discomfort because of external wounds, such as cuts or burns, they may not notice them. Infection can happen if the injury is not treated right way. In diabetic patients, non-healing wounds can lead to complications like gangrene, osteomyelitis, abscess, cellulitis, etc. Although the pathophysiology of diabetes does not directly link impaired wound healing to this disease, some molecular factors (including vascular endothelial growth factors) have been demonstrated to enhance this process in diabetic rats (Stino *et al.,* 2020).

The nanofibrous scaffold mimics the environment in which tissues are formed in nature. Because of its large surface-to-volume ratio, this scaffold promotes cell adhesion, proliferation, and differentiation more effectively than other available variants. Different techniques are used to make them, such as phase separation, self-assembly, melt blowing, and electrospinning. Nanofibrous scaffolds can be fabricated using electrospinning for wound healing, drug delivery, and tissue engineering (Anjum *et al.,* 2022). In wound healing, nanofibrous scaffolds protect the injured area from moisture loss, help in removal of exudates, and inhibit microbe invasion. Nanofibrous scaffolds have special properties that promote faster wound healing, especially in chronic wounds like diabetic ulcers (Palanisamy *et al.,* 2020).

Nanomaterials such as fibers or capsules are generated without high temperatures or pressures. The electrospinning has gained considerable interest in encapsulating bioactive compounds over past few years (Palanisamy *et al.,* 2022). Polymeric solutions containing proteins and polysaccharides are used to electrospun fibers. The versatility, biodegradability, low cost, and abundance of starch make it a popular ingredient in food industry. Studies have been conducted using starches with high amylose content or in combination with synthetic polymers to produce electrospun fibers from starch.

Fox grape *Cayratia trifolia* (voucher No. BSI/SRC/5/23/2010-2011/Tech.1527) is a medicinal plant which belongs to the family *Vitaceae* (Perumal *et al*., 2014). Preliminary phytochemical analyses revealed that the whole plant of *C. trifolia* contains waxy oil, steroids, terpenoids, flavonoids, and tannins. In addition to stilbenes, *C. trifolia* leaves contain piceid, reveratrol, viniferin, and ampelopsin (Sowmya *et al.,* 2021). The stem, leaves, and roots also reportedly contain delphinidin in addition to hydrocyanic acid. It is possible to prepare a decoction of roots by mixing them with coconut oil. Ground roots can be combined with black pepper to form a poultice for boils (Perumal *et al.,* 2016). The traditional method of monitoring diabetes patients' blood sugar levels involves infusing seeds with extracts from tubers. Snake bites are treated with a paste made from tubers (Sowmya *et al.,* 2015). In tumour, neuralgia, and splenopathy, the whole plant is regarded as a diuretic. Studies conducted with animal models have shown that the bark extract of *C. trifolia* has antioxidant, antiviral, antibacterial, antiprotozoal, hypoglycaemic, anticancer, and wound healing properties (Perumal *et al*., 2015; Meganathan *et al*., 2021; Palanisamy *et al*., 2021). So far, starch fibers have not been used to encapsulate linolenyl alcohol bioactive compound by electrospinning for wound healing applications. Thus, the aim of present study was to encapsulate linolenyl alcohol in electrospun starch-based nanofibrous scaffolds and test their wound healing capabilities.

MATERIALS AND METHODS

The immortalized human keratinocytes (HaCat) cells used in the study were acquired from American Type Culture Collection (ATCC). Dulbecco's modified Eagle medium (DMEM) and fetal bovine serum (FBS) were sourced from Thermo Fisher Scientific Inc., along with 3,4,5-dimethylthiazol-2-

yl-2,5-diphenyltetrazolium bromide (MTT) reagent and bovine serum albumin (BSA). Santa Cruz Biotechnology Inc. furnished the mouse monoclonal anti-VEGF antibody, while Sigma-Aldrich supplied the rabbit polyclonal anti-PDGF receptor antibody. Starch, ethanol, acetic acid and phosphate buffered saline (PBS) were obtained by Merck Company.

Preparation of polymeric solutions for electrospinning

Using soluble potato, the starch in formic acid, polymeric solutions were prepared. A solution of formic acid and deionized water was prepared by dissolving 5 g starch in 10 mL deionized water. Starch gelatinization was achieved by stirring the solutions at 150 rpm for 24 h and allowing them to age for another 24 h. Various polymeric solutions were prepared by replacing 0, 10, 20 and 40% starch with linolenyl alcohol (Meganathan and Panagal, 2023) in dry bases (0, 10, 20 and 40%, v/v) and stirred for 15 min, followed by electrospinning. In control treatment linolenyl alcohol was not added to the starch solution. To ensure the complete dissolution of polymers, the polymeric solutions were sealed and aged for 24 h at room temperature before electrospinning. For solution characterization**,** Brookfield Model DV-II + Pro Viscometer and a Metrohm-914 conductometer were used to determine the viscosity and conductivity of the prepared four solutions prior to electrospinning.

Electrospinning process

A syringe infusion pump (KD Scientific, Model 100, Holliston, England) and an electrospinning apparatus were used to produce starch nanofibers for encapsulation of linolenyl alcohol. Using a 3 mL plastic syringe fitted with a stainless-steel spinneret needle of 0.7 mm diameter, the fiber-forming solution was loaded 20 cm from a grounded stainless-steel collector plate. Electrospun nanofibers were generated at room temperature (25$\pm$2°C) with a relative humidity set to 45$\pm$2°C and a dehumidifier to maintain the humidity. As the solution was pumped at a steady flow rate of 0.6 mL h^{-1} and an applied voltage of +25.0 kV and –3.0 kV. To eliminate impurities and keep the nanofibrous sheets at 25°C for drying, the sheets were rinsed thrice with water and phosphate buffer solution (PBS).

Physicochemical characterization of fabricated nanofibers

A scanning electron microscope (SEM, Jeol, JSM-6610LV, USA) was used to analyse nanofiber morphology. A voltage acceleration of 10 kV was used to analyse the samples after they were sputter-coated with gold. Using, we calculated The size distribution and average diameter of 50 randomly selected nanofibers were calculated from SEM micrographs by using ImageJ software (2015 version). The thermos-gravimetric analyser (TGA, TA-60WS, Shimadzu, Kyoto, Japan) was used to determine the thermal stability of fabricated nanofibers. In platinum capsules, the samples of 5 mg had a heating rate of 10°C min^{-1} in a range of 30-600°C and nitrogen flow of 50 mL min^{-1}. As a reference, an empty platinum capsule was used. An attenuated total reflection (ATR) accessory (IR-affinity, Shimadzu, Japan) was used to obtain the infrared spectrum of fabricated nanofibers and their constituents (soluble potato starch and linolenyl alcohol). In analysis, 120 scans were made at a spectral resolution of 4 cm for a wavenumber range of 4000-500 cm at room temperature (25$\pm$2°C).

Biological characterization of fabricated nanofibers

Cell viability analysis: For cell culture**,** HaCat cells were maintained at 37°C during experimentation in a humidified atmosphere containing 5% CO_2**.** In T-25 flasks, the cells were grown in DMEM supplemented with 10% FBS and 1% antibiotics (100 U mL^{-1} penicillin and 100 g mL^{-1} streptomycin). Once the cells reached 70% confluence, they were trypsinized and passaged. For cell viability and proliferation, MTT assay was done as per the standard test method (Lavanya *et al.*, 2023). Electrospun nanofibrous mats were assessed for *in vitro* cytotoxicity. For sterilization, the specimens were immersed in 70% ethanol for 30 min and then washed with PBS in sterile conditions. HaCat cells were cultured in 96-well plates with a density of 5×10^3 cells per well in DMEM supplemented with 10% FBS and 1% antibiotics (100 U mL^{-1} penicillin and 100 g mL^{-1} streptomycin). The culture plates were maintained at 37°C and 5% CO_2 for 24 h. The viability of cultured cells was determined by colorimetric MTT assay using ELISA Reader ELX 808 at 540 nm based on optical density detection.

Scratch assay (in vitro wound healing)

DMEM supplemented with 10% FBS was used to extract nanofibrous mats after they were sterilized and placed in 2 mL DMEM for 24 h. 12-well plates were used to grow HaCat cells at concentration of 2.5 x 10^5 cells per well. They were placed in an incubator wherein they formed a monolayer of cells in each well. To form a cell-free area in each well, a sterile 200 µL pipette tip was used to scratch the surface of cell layer. The cell layer was washed with PBS to remove non-adhered cells. Finally, the prepared extracts of each specimen were added to the culture plates with scratch and kept at 37°C in 5% CO_2. Optical microscopes (Motic BA310E) were used to monitor the migration of cells between scratch areas (from the wound edges to fill the gap) after 0 and 24 h. ImageJ software was used to measure the wound gap area at the start point and after 24 h.

Protein expression analysis by western blotting

SDS-PAGE was used to separate proteins using sodium dodecyl sulfate-polyacrylamide gel electrophoresis. The sample mixtures were heated at 95°C for 4 min, and then cooled on ice using equal volumes (50 g) of samples and buffer. Following the separation of proteins with a Bio-Rad mini slab gel apparatus at a constant voltage of 100 volts, the dye front was reached at the bottom of the running gel. In this experiment, polyvinylidene difluoride (PVDF) membranes were charged at a constant voltage of 100 V for 1 h to transfer protein bands. A primary antibody incubation was performed with anti-VEGF (mouse monoclonal antibody 200 g mL^{-1}) and anti-PDGF (rabbit polyclonal antibody 100 g mL^{-1}) at appropriate dilutions followed by blocking with 5% BSA blocking solution at room temperature for 1 h at appropriate dilutions. In addition to the primary antibody, a secondary antibody [goat anti-mouse monoclonal antibody, 400 g mL^{-1}, was purchased from Santa Cruz Biotechnology, Inc.] and 1:10,000 was incubated for 1 h after the the incubation of primary antibody. After incubation with secondary antibody, the cells were washed twice for 5 min each with tris-buffered saline, tween (TBS-T), and placed on Saran WrapTM (protein side up). Immediately after the addition of detection reagent mixture to the blot, the blots were incubated for 30-60 sec and excess reagent drained off (ECL). The immunoblot signals were quantified using Quantity One 1-D Analysis Software (Bio-Rad). In the presence of a probe that consisted of β-actin, similar amounts of proteins were loaded onto the membranes.

Statistical analysis

The data are presented as mean ± standard deviation (SD). Statistical t-test was used to compare the differences between the two groups, considering a p value < 0.05 as significant.

RESULTS AND DISCUSSION

Solution characterization

Before electrospinning, polymeric solution properties such as viscosity and conductivity were measured to correlate with electrospinning results. Different polymeric solutions were prepared with different compositions and the solutions with higher linolenyl alcohol content (C and D) showed a higher viscosity and conductivity (Fig. 1 and 2). Increased viscosity increased the inter- and intra-molecular H bonding between starch and linolenyl alcohol, thereby decreasing the surface tension and forming uniform fibers. As a result of high interactions and chain entanglement between starch and linolenyl alcohol, the addition of starch content increased the viscosity of solutions. Since starch contains 25% amylase, therefore linolenyl alcohol can be linked with amylase, which is a long linear polymer composed of 1,4-glucopyranoside.

Physicochemical characterization of fabricated nanofibers

Morphology and size distribution: The nanofibers were fabricated with different morphologies and sizes (Fig. 3). A ribbon-shaped and fused morphology was observed for the nanofibers without linolenyl

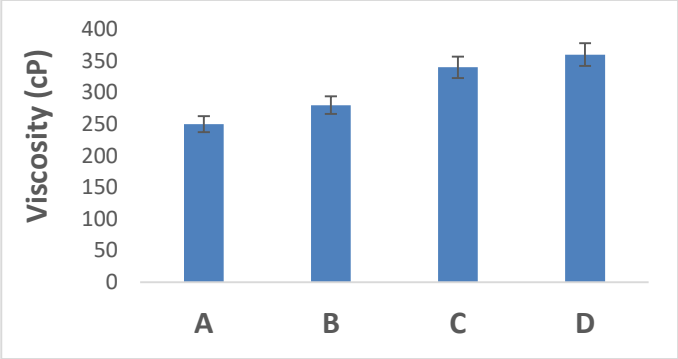

Fig. 1: Viscosity of fabricated nanofibers. A) 0% linolenyl alcohol, B) 10% linolenyl alcohol, C) 20% linolenyl alcohol and D) 40% linolenyl alcohol

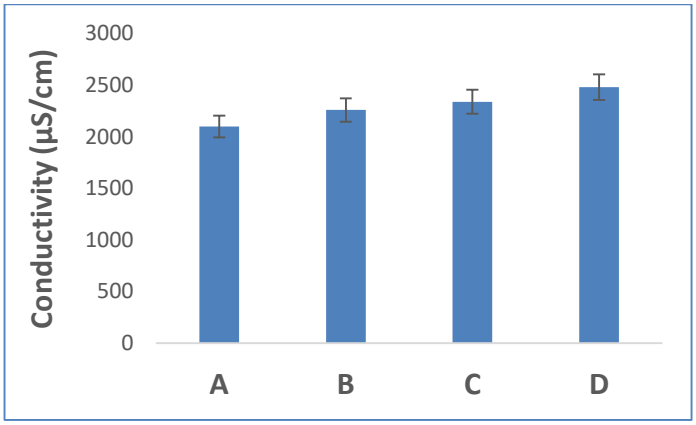

Fig. 2: Conductivity of fabricated nanofibers. A) 0% linolenyl alcohol, B) 10% linolenyl alcohol, C) 20% linolenyl alcohol and D) 40% linolenyl alcohol

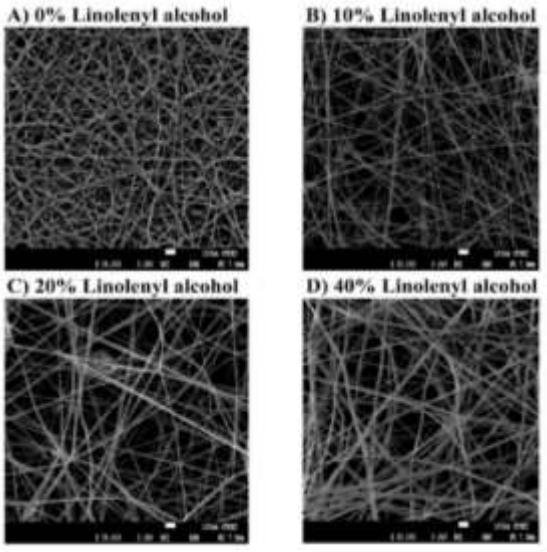

Fig. 3: Morphology of fabricated starch nanofibers loaded with linolenyl alcohol

alcohol. Because the solution is not stretched during electrospinning, this is the case. In contrast, nanofibers with linolenyl alcohol (the average diameter of nanofibers were 96, 72, 83 and 94 nm for 0, 10, 20 and 40% of linolenyl alcohol, respectively) were homogeneous, cylindrical, and. randomly oriented, suggesting that the solvent was volatilized more rapidly. High-concentration fiber-forming solutions require a long tip-to-collector distance and high voltage to align starch molecules in the jet (Kong and Ziegler, 2013). A relatively high starch concentration (50% w/v) was used in this study, however, the solution did not exhibit high viscosity in formic acid solvent. Further, the starch solution became more electro-spinnable after linolenyl alcohol was added. Recent research has produced ultrafine fibers from soluble potato starch with beaded-fiber morphologies and average diameters ranging from 128 to 143 nm (Fonseca *et al.*, 2019). To produce bead-less nanofibers with a diameter of 72 to 96 nm, the parameters of the solutions and electrospinning process conditions were altered in this study. It is possible that these nanofibers could be used in wound healing applications to release linolenyl alcohol-controlled releases.

Thermal stability of nanofibers

Thermal stability of nanofibers was determined using thermogravimetric analysis (TG). A weight loss thermogram and a first derivative thermogram are shown in Fig. 4. Nanofibers without linolenyl alcohol (0%) showed similar weight loss behaviour to pure soluble potato starch. Moisture evaporation occurs at approximately 100°C, followed by starch decomposition at 250–300°C. Compared to linolenyl alcohol's boiling point (around 374°C), the free linolenyl alcohol exhibited one-step weight loss at 160°C. There were three stages of

weight loss for nanofibers with linolenyl alcohol (10, 20 and 40%); the first stage was due to moisture evaporation at 100°C. At around 200-250°C, the second stage was likely caused by linolenyl alcohol degradation. During the third stage, starch decomposition occurred between 250 and 300°C. Based on these results, linolenyl alcohol was successfully encapsulated in starch fibers, and the nanofibers that were loaded with linolenyl alcohol were more thermally stable.

Fig. 4: Thermogravimetric analysis of starch nanofibers loaded with linolenyl

Fig. 5: FT-IR spectrum of starch nanofibers loaded with linolenyl alcohol

Fourier-transform infrared (FT-IR) spectroscopy analysis of nanofibers

FT-IR spectra for nanofibers and constituents are presented in Fig. 5. The characteristic bands can be attributed to the stretching vibrations of free inter- and intra-molecular bound hydroxyl groups in soluble potato starch. The bands at 2941 cm^{-1} is due to the bond H C single stretching, bands at 1641 cm^{-1} is due to water in the starch. The bands at 1351 cm^{-1} represents C single bond O single bond H bending or CH_2 deformation. The bands at 1153 and 1020 cm^{-1} can be attributed to the stretch of a single bond as well as a double bond. The band around 920 cm^{-1} is most likely due to the glycosidic bonds that glucose contains. Functional group characteristic of linolenyl alcohol, absorption band at 1728 cm^{-1} for a carbonyl group and a shoulder peak at 2858 cm^{-1} for an aldehyde

hydrogen group (CHO). The bands at 2924 cm^{-1} is due to C-H stretching and the bands at 1458 and 1381 cm^{-1} are due to C-H bending bonds. The band at 1529 cm^{-1} may be due to the C=C group.

Biological characterization of fabricated nanofibers

Cell viability: Ideal wound dressing is expected to be highly compatible. A MTT test was performed on electrospun nanofibrous mats after their exposure to human keratinocytes (HaCat cells) for 24 and 48 h, respectively (Fig. 6). Test revealed that electrospun nanofibrous mats were viable and cytocompatible cells. After 24 h, the nano-fibrous mats showed 100-130% cell viability as compared to control. Within 48 h of contact with HaCat cells, all mats had a cell viability of 100-160%. Starch-incorporated nano-fibrous mats showed higher cell viability than those without starch. It revealed that nano-fibrous mats developed for tissue engineering were highly compatible.

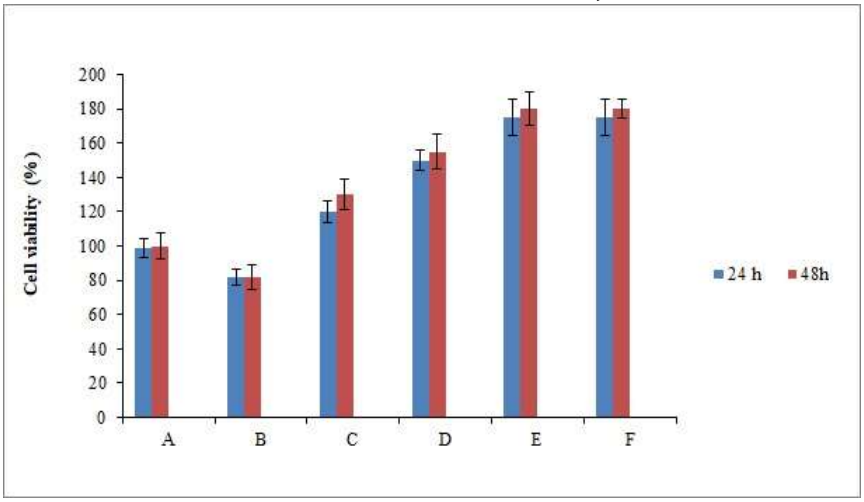

Fig. 6: Cell viability of fabricated nanofibers on HaCat cells for 24 and 48 h of treatment. A) Control, B) 100% linolenyl alcohol, C) 0% linolenyl alcohol, D) 10% linolenyl alcohol, E) 20% linolenyl alcohol and F) 40% linolenyl alcohol

Scratch assay (in vitro wound healing)

An *in vitro* wound healing analysis based on cell migration was performed by scratch assay using a simple and low-cost methodology. To regenerate the new dermal structure, wound

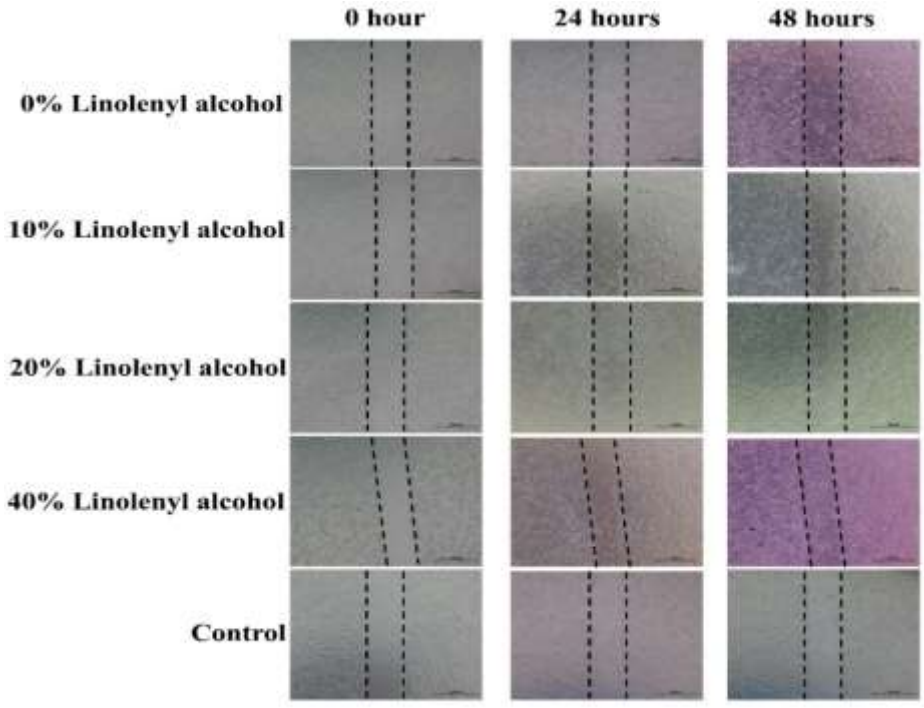

Fig. 7: Fabricated nanofibers wound healing micrographs and cell migration into the scratch area after 24 and 48 h

healing involves migration and growth of cells as well as a variety of growth factors. In this study, HaCat cells were examined for migration from side to side of artificial wounds after 24 and 48 h. The migration of cells to the scratched area in 24 and 48 h period is given in Fig. 7. The MRI Wound Healing Tool of ImageJ software was used to determine the kinetics of wound healing. As an indication of wound healing capability, the fabricated nanofibers demonstrated wound closure efficiency (Fig. 8). Additionally, the mat demonstrated excellent wound healing of 100%, proving its high biocompatibility and suitable wound closure properties.

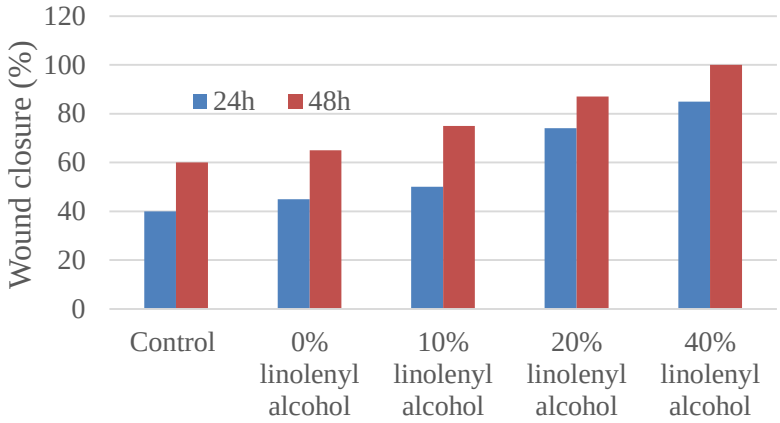

Fig. 8: Wound closure efficiency of fabricated nanofibers on HaCat cells

Protein expression analysis

The effect of nanofibers on the expression of VEGF and PDGF proteins in HaCat cells. HaCat cells were incubated in DMEM supplemented with 10% FBS for 24 h with fabricated nanofibers at test concentrations. Protein expression was calculated using densitometry analysis, which is expressed as relative intensity. This study performed internal controls using β-actin. Each bar represents the mean and standard error of mean based on five independent observations. Student's–Newman-Keul's test was used to determine significance. VEGF and PDGF expression levels comparatively increased at fabricated starch nanofibers loaded with 40% linolenyl alcohol (Fig. 9). Wound healing is stimulated by VEGF through a variety of mechanisms, such as collagen deposition,

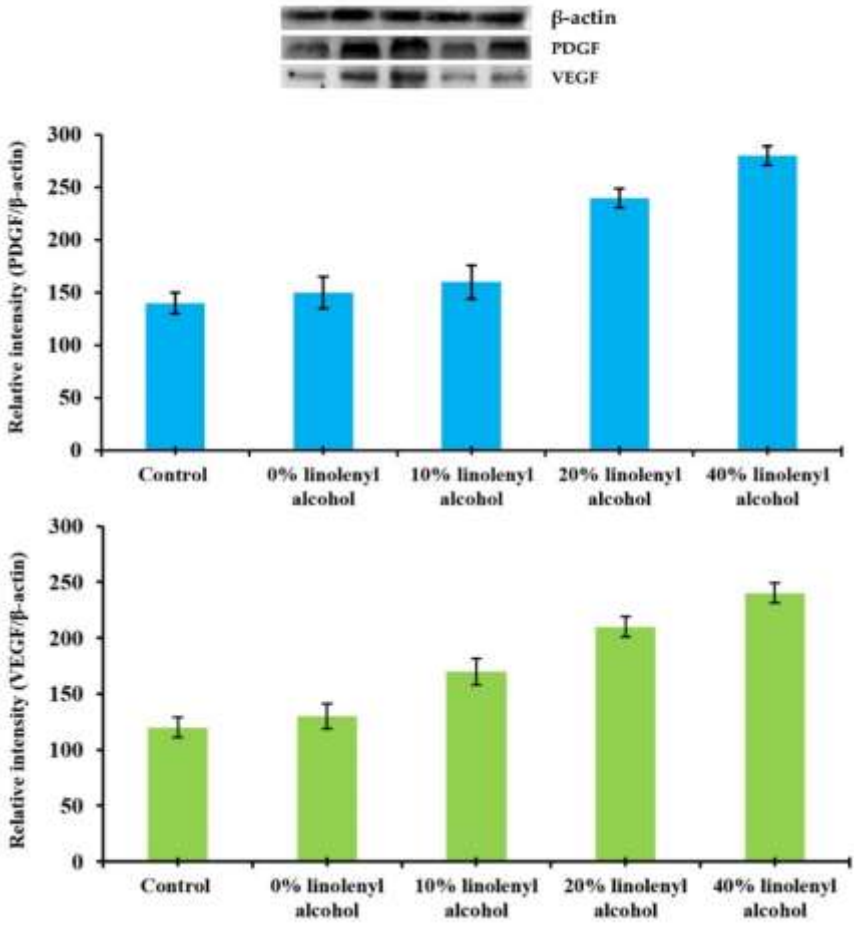

Fig. 9: Effects of fabricated nanofibers on VEGF and PDGF protein expression in HaCat cells

angiogenesis, and epithelization. VEGF's mitogenic, chemotactic, and permeability effects may help in promoting wound healing in arterial occlusive disease and diabetes patients with non-healing wounds. Moreover, it may alleviate the "wound" of ischemic heart disease. Perfusion of tissue is improvedby VEGF's ability to promote angiogenesis. On the other hand, PDGF stimulate the synthesis of DNA and chemotaxis of fibroblasts and smooth muscle cells and stimulates the production of collagen, glycosaminoglycan, and collagenase by fibroblasts. *In vitro* results suggest that PDGF delivered by platelets to the site of injury in vivo may play a significant role in wound healing. Epidermal growth factor alone or in combination with PDGF resulted in thickening of epidermis. PDGF modulates wound healing by interacting synergistically with other factors (Bao *et al.*, 2009). In this study, fabricated starch nanofibers loaded with 40% linolenyl alcohol increased the expression level of VEGF and PDGF suggesting that, the fabricated nanofibers promote the wound healing process via VEGF and PDGF signalling pathways.

Conclusion: The study focussed on to develop novel electrospun fabricated starch nanofibers loaded with linolenyl alcohol for application in wound dressings containing different compositions of starch and linolenyl alcohol. SEM confirmed that the fabricated nanofibers had uniform morphology without beads and well-designed and interconnected pores. Functional groups of components were detected by FTIR in composite nanofibers. Cell growth and proliferation studies revealed that electrospun nanofibers were cytocompatible, confirming their cytocompatibility as wound dressings. Fabricated nanofibers enhanced *in vitro* wound healing efficiency due to cell growth and migration to cover up the wound gap area in scratch assay. It also increased the level of VEGF and PDGF proteins in HaCat cells in western blot analysis. These findings suggest that electrospun fabricated starch nanofibers loaded with linolenyl alcohol have a significant impact on accelerating wound healing.

Acknowledgement: The authors express their sincere gratitude to the Department of Biotechnology, Annai College of Arts and Science, Kumbakonam, Tamil Nadu, India for providing facilities for this research work in such a fine manner.

REFERENCES

Anjum, S., Rahman, F., Pandey, P., Arya, D.K., Alam, M., Rajinikanth, P.S. and Ao, Q. 2022. Electrospun biomimetic nanofibrous scaffolds: A promising prospect for bone tissue engineering and regenerative medicine. *International Journal of Molecular Sciences*, **23**(16): 9206. [*https://doi.org/10.3390/ijms23169206*].

Bao, P., Kodra, A., Tomic-Canic, M., Golinko, M.S., Ehrlich, H.P. and Brem, H. 2009. The role of vascular endothelial growth factor in wound healing. *Journal of Surgical Research*, **153**(2), 347-358.

Fonseca, L.M., Silva, F.T., Antunes, M.D., El Halal, S.L.M., Lim, L. and Dias, A.R.G. 2019. Aging time of soluble potato starch solutions for ultrafine fibers formation by electrospinning. *Starch – Stärke*, **71**: 1-7.

Kong, L. and Ziegler, G.R. 2013. Quantitative relationship between electrospinning parameters and starch fiber diameter. *Carbohydrate Polymers*, **92**(2): 1416-1422.

Lavanya, M., Krishnamoorthy, R., Alshuniaber, M.A., Manoharadas, S., Palanisamy, C.P., Veeraraghavan, V.P., Jayaraman, S., Rajaaagopal, P. and Padmini, R. 2023. Formulation, characterization and evaluation of gelatin-syringic acid/zinc oxide nanocomposite for its effective anticancer, antioxidant and anti-inflammatory activities. *Journal of King Saud University Science*, **35**(8): 102909. [*https://doi.org/10.1016/j.jksus.2023.102909*].

Meganathan, B. and Panagal, M. 2023. Wound healing potential of bioactive compound from *Cayratia trifolia* (L.): An *in silico* and *in vitro* analysis. *Biological Forum*, **15**(5): 104-113.

Meganathan, B., Palanisamy, C.P. and Panagal, M. 2021. Antioxidant, antimicrobial and cytotoxicity potential of n-hexane extract of *Cayratia trifolia* L. *Bioinformation*, **17**(3): 452. [*https://www.ncbi.nlm.nih.gov/pmc/articles/PMC8131575/*].

Palanisamy, C.P., Alugoju, P., Jayaraman, S. and Poompradub, S. 2023. *Nigella sativa* L. seed extracts promote wound healing progress by activating VEGF and PDGF signaling pathways: An *in vitro* and *in silico* study. *F1000Research*, **12**: 436. [*https://doi.org/10.12688/f1000research.132106.10*].

Palanisamy, C.P., Cui, B., Zhang, H., Gunasekaran, V.P., Ariyo, A.L., Jayaraman, S., Rajagopal, P. and Long, Q. 2022. A critical review on starch-based electrospun nanofibrous scaffolds for wound healing application. *International Journal of Biological Macromolecules*, **222**: 1852-1860.

Palanisamy, C.P., Cui, B., Zhang, H., Jayaraman, S. and Muthukaliannan, G.K. 2020. A comprehensive review on corn starch-based nanomaterials: Properties, simulations, and applications. *Polymers*, **12**(9): 2161. [*https://www.mdpi.com/2073-4360/12/9/2161*].

Palanisamy, C.P., Pethanan, S., Vincent, G.G., Murugesan, K., Ramachandran, A., Sivanandam, R. and Panagal, M. 2021. Chemotherapeutic potential of *Cayratia trifolia* L. n-hexane extract on A2780 cells. *Bioinformation*, **17**(8): 710. [*https://www.ncbi.nlm.nih.gov/pmc/articles/PMC9049100/*].

Pei, J., Palanisamy, C.P., Alugoju, P., Anthikapalli, N.V.A., Natarajan, P.M., Umapathy, V.R., Swamikannu, B., Jayaraman, S., Rajagopal, P. and Poompradub, S. 2023. A comprehensive review on bio-based materials for chronic diabetic wounds. *Molecules*, **28**(2): 604. [*https://doi.org/10.3390/molecules28020604*].

Pei, J., Prasad, M., Mohamed Helal, G., El-Sherbiny, M., Abdelmonem Elsherbini, D.M., Rajagopal, P., Palanisamy, C.P., Veeraraghavan, V.P., Jayaraman, S. and Surapaneni, K.M. 2022. Beta-sitosterol facilitates GLUT4 vesicle fusion on the plasma membrane via the activation of Rab/IRAP/Munc 18 signaling pathways in diabetic gastrocnemius muscle of adult male rats. *Bioinorganic Chemistry and Applications*, **2022**: 7772305. [*https://doi.org/10.1155/2022/7772305*].

Perumal, P.C., Reddy, C.P.K., Pratibha, P., Sowmya, S., Priyanga, S., Devaki, K., Ramkumar, S. and Gopalakrishnan, V.K. 2015. CXCR4 inhibitory activity analysis of linoleic acid isolated from ethanolic extract of *Cayratia trifolia* (L.): An molecular docking simulation. *International Journal of Pharmacognosy and Phytochemical Research*, **7**(4): 781-784.

Perumal, P.C., Sowmya, S., Pratibha, P., Vidya, B., Anusooriya, P., Starlin, T. and Gopalakrishnan, V. K. 2014. Identification of novel PPARγ agonist from GC-MS analysis of ethanolic extract of *Cayratia trifolia* (L.): A computational molecular simulation studies. *Journal of Applied Pharmaceutical Science*, **4**(9): 6-11.

Perumal, P.C., Sowmya, S., Velmurugan, D., Sivaraman, T. and Gopalakrishnan, V.K. 2016. Assessment of dual inhibitory activity of epifriedelanol isolated from *Cayratia trifolia* against ovarian cancer. *Bangladesh Journal of Pharmacology*, **11**(2): 545-551.

Sowmya, S., Perumal, P.C., Anusooriya, P., Vidya, B., Pratibha, P. and Gopalakrishnan, V.K. 2015. *In vitro* antioxidant activity, *in vivo* skin irritation studies and HPTLC analysis of *Cayratia trifolia* (L.) Domin. *International Journal of Toxicological and Pharmacological Research*, **7**(1), 1-9.

Sowmya, S., Perumal, P.C., Ravi, S., Anusooriya, P., Shanmughavel, P., Murugesh, E., Chaithanya, K.K. and Gopalakrishnan, V.K. 2021. 1-pentacosanol isolated from stem ethanolic extract of *Cayratia trifolia* (L.) is a potential target for prostate cancer - *In silico* approach. *Jordan Journal of Biological Sciences*, **14**(2). [*https://jjbs.hu.edu.jo/files/vol14/n2/paper%20number%2023.pdf*].

Stino, A.M., Rumora, A.E., Kim, B. and Feldman, E.L. 2020. Evolving concepts on the role of dyslipidemia, bioenergetics, and inflammation in the pathogenesis and treatment of diabetic peripheral neuropathy. *Journal of the Peripheral Nervous System*, **25**(2): 76-84.

Xu, Z., Han, S., Gu, Z. and Wu, J. 2020. Advances and impact of antioxidant hydrogel in chronic wound healing. *Advanced Healthcare Materials*, **9**(5): 1901502. [*https://doi.org/10.1002/adhm.201901502*].